Q_0 defines the sensitivity of a point-like absorber placed at a scattering angle ξ = 90° and is represented as:

$$Q_0 = \frac{1+\alpha}{1+\alpha+\alpha^2} \tag{2.35}$$

with $\alpha = \frac{E_\gamma(keV)}{511}$. Once the sensitivity as a function of the incident γ-ray energy is known, the linear polarization of the γ rays can be directly found by using the asymmetry measurement. The value of sensitivity increases as the distance between a scatterer and an absorber increases because the solid angle decreases, but due to a decrease in the solid angle, the coincidence efficiency becomes lower. Thus, the overall quality of a Compton polarimeter depends on both coincidence efficiency as well as sensitivity [101].

2.13.2 Mixing Ratio Calculation via R_{DCO} -Polarization Method

This method is an alternative to the angular distribution method for determining the mixing ratio of γ-transitions. In this method, the theoretical value of R_{DCO} and linear polarization are calculated by varying δ within a range of -50 to 50, having intervals. The theoretical value of R_{DCO} is calculated by using the ANGCOR code [95], and the theoretical value of polarization can be calculated by using equations 2.25 and 2.26. Then a contour plot of R_{DCO} and polarization is obtained for different values of δ. The experimental value of R_{DCO} and polarization of the observed transition are then compared with the theoretical values. To observe the value of δ, the standard deviation χ^2 values (between the measured and calculated values) are plotted with respect to δ, and then that value of δ is considered for which the χ^2 is minimum.

Chapter 3

Nuclear Models

The atomic nucleus is a highly complex and dynamic system; despite decades of research, an unified all-encompassing theory that explains the nuclear structure in all its intricacies remains elusive. This is primarily because the behavior of the nucleus cannot be fully captured by a single model. Different nuclear models are necessary to describe various aspects of nuclear structure, as each model offers unique perspectives on how nucleons (protons and neutrons) interact within the nucleus. The complexity of the nucleus arises from several factors, including the interplay between nuclear forces, the collective motion of nucleons, and the quantum nature of subatomic particles. Additionally, the nucleus exhibits a variety of configurations, such as spherical, deformed, and collective rotational structures, making it difficult for a single model to describe all of these behaviors adequately. Therefore, a large number of nuclear models have been developed, each suited to specific situations or types of nuclei.

3.1 Various Modes of Excitation

As we have discussed in the introduction, the nucleus can generate angular momentum via two mechanisms: non-collective single-particle excitations and collective rotation. These two modes will be explained briefly in this chapter.

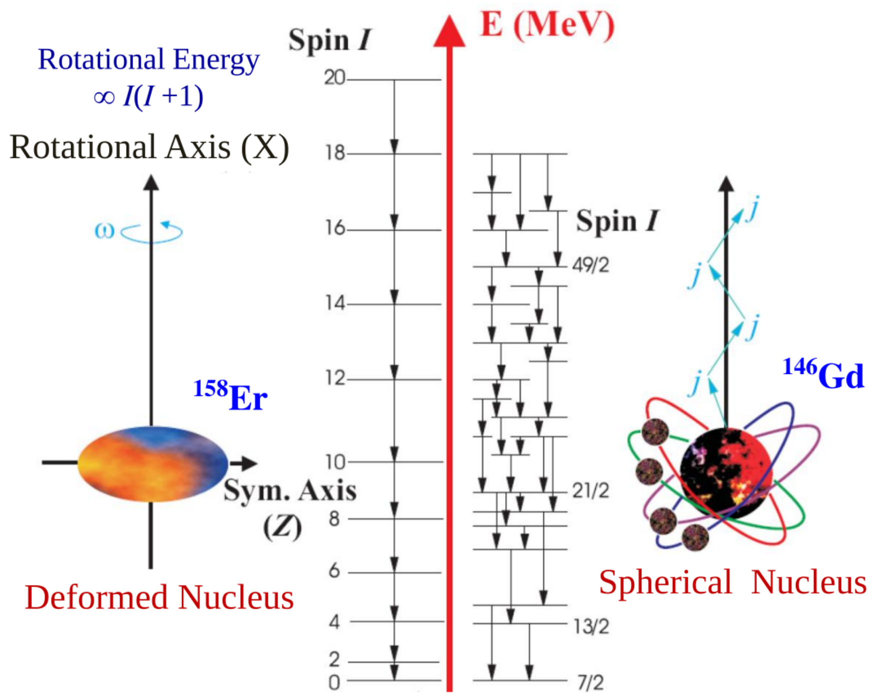

Figure 3.1 Angular momentum generation via collective rotation in deformed ^{158}Er nucleus and through single-particle excitation in nearly-spherical nucleus ^{146}Gd [3, 71].

3.1.1 Single Particle Excitation

This type of excitation exists in those nuclei that are near closed shells (2, 8, 20, 28, 50, 82, 126). These kinds of nuclei generate angular momentum by rearranging their valence nucleons in different orbitals. In Fig. 3.1, an example of such a type of excitation is shown (right panel). The total angular momentum is the sum of the individual angular momenta of valence nucleons that are not coupled to spin zero. The bulk of the nucleons form the core make no contribution to the angular momentum generation. When a pair is broken to excite a particle from the ground state, a hole remains in the previously occupied level. In the presence of pairing, the single-particle and hole excitations are no longer the fundamental excitations. Instead, quasi-particle energy can be viewed as a generalized form of single-particle and hole excitation energies. The pairing interaction Hamiltonian can be written as:

$$\hat{H}_{pair} = \sum_{k,k'} (G_{k,k'} \hat{\Phi}_k^{\dagger} \hat{\Phi}_{k'}) \tag{3.1}$$

where, $\hat{\Phi}_k$ is the quasiparticle field operator for the single-particle state and $G_{k,k'}$ is the pairing interaction strength. The quasi-particle energy is defined as

$$E_{qp} = \sqrt{(\varepsilon_i - \lambda)^2 + \Delta^2} \tag{3.2}$$

where ε_i is the single-particle energy of the state, λ is the Fermi level energy, and Δ is the strength of the pairing interaction. Thus, the particles and holes are replaced by quasi-particles representing partially filled levels. This transformation from particles to quasi-particles greatly simplifies the shell model calculation, as the quasi-particle excitations relative to the Fermi surface are considered.

3.1.2 Collective Rotation

The nuclei, which have an axially deformed shape rather than a spherical one, can produce angular momentum by collective rotation. The rotation occurs perpendicular to the symmetry axis, and all nucleons contribute coherently to the angular momentum. The total angular momentum I, in this case, can be obtained by combining the angular momentum of the core R, and the sum of the single-particle contributions

$$I = \sum_i j$$

The characteristic signature of this mode of excitation is the observation of regular band sequences in the level scheme (left panel of Figure 3.1) with rotational energy proportional to $I(I + 1)$, I being the spin of the state [2]. The energy of a transition in a rotational band is defined as:

$$E_\gamma = E(I) - E(I-2) = \frac{\hbar^2}{2\mathscr{J}}(4I-2) \tag{3.3}$$

where $\mathscr{J}$ represent the moment of inertia. The higher angular momentum states are generated by exciting the particle into a higher orbital, *i.e.*, with higher excitation energy. The alignment of the quasi-particles prefers the angular momentum vector oriented along either the symmetry axis or rotational axis, depending on the nuclear shape of the core (prolate or oblate) and the nature of the quasi-particle (hole or particle), as shown in Fig. 3.2. Such orientation depends on the overlap of the quasi-particle with the mass distribution of the core, as discussed in the introduction section.

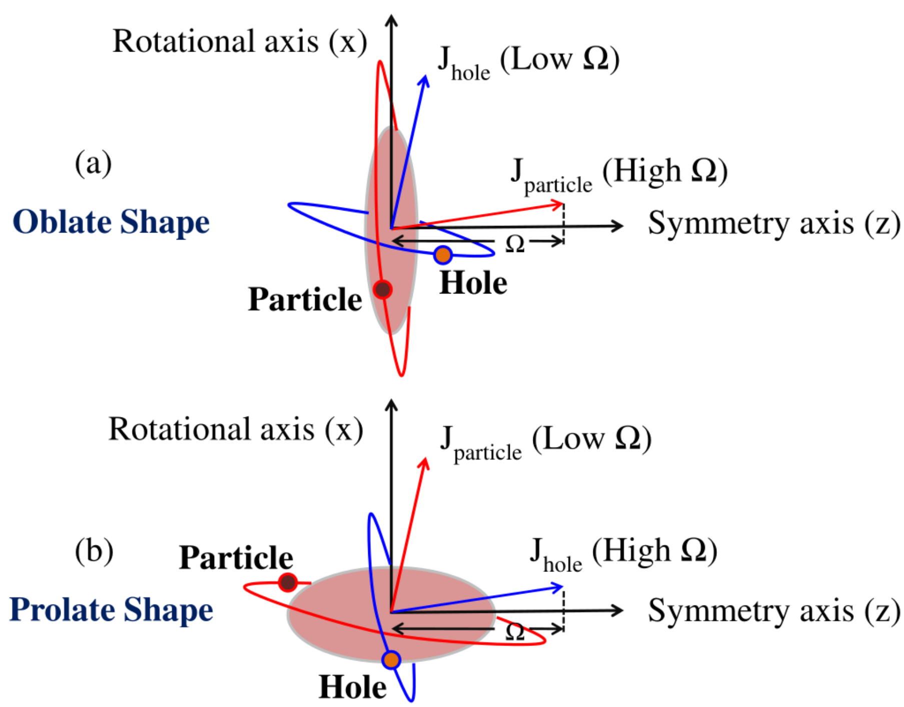

Figure 3.2 Alignment of the particle-hole angular momentum in case of oblate (a) and prolate (b) shapes. Ω represents the projection of the angular momentum along the symmetry axis [71].

The collective model does not include the effects of a pairing force; it only deals with the Coriolis force and the deformed nuclear field. The Coriolis force may not be sufficiently strong enough to influence the valence nucleon's motion at low rotational frequency. In the presence of a sufficient deformed nuclear field, the motion of all the nucleons will be coupled to the deformation of the core at low frequency, as shown in Fig. 3.3, this type of coupling is known as a strong coupling limit and the valence nucleon's angular momentum will subsequently be aligned with the symmetry axis.

As the rotational frequency of a nucleus increases, the Coriolis force becomes strong enough to break the pairs of nucleons. The nucleon's motion can be coupled to the rotation of the core, as shown in Fig. 3.3, causing the angular momentum to align along the rotation axis. The energy of the Coriolis force can be expressed as [102],

$$E_{Cor} = \frac{\hbar^2}{\mathscr{J}} I.j \tag{3.4}$$

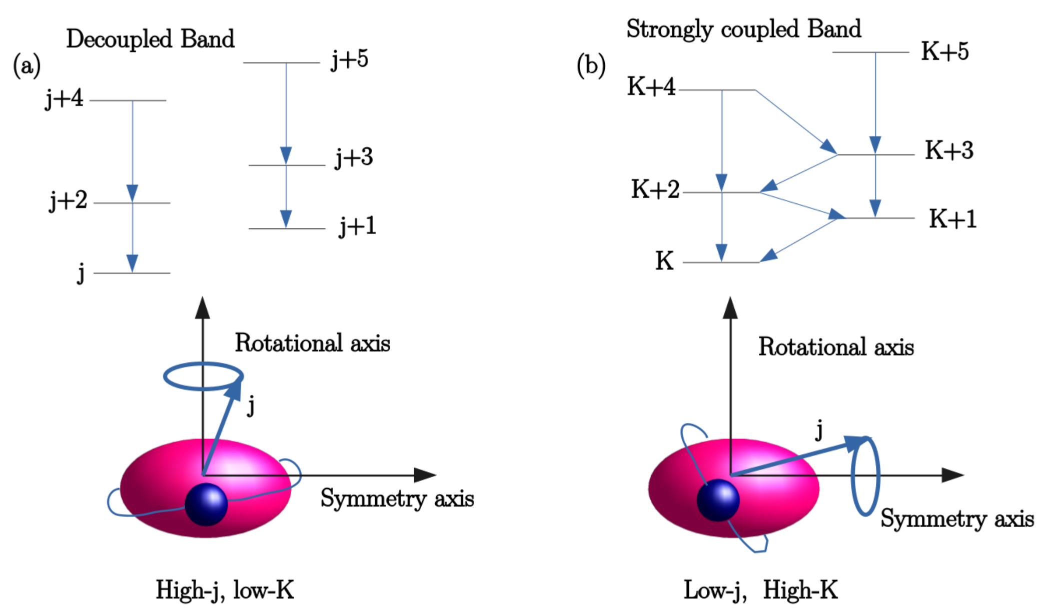

Figure 3.3 Angular momentum Coupling scheme for the deformed nuclei in the Strong(deformation aligned) and Weak (rotational alignment) coupling limits. K represents the projection of total angular momentum on the symmetry axis.

where I and $\mathscr{J}$ are the total angular momentum of the valence nucleon and the moment of inertia of the core, respectively. From the above equation, it is clear that the high j particle will be aligned first. When a pair of nucleons separate, nucleus angular frequency decreases due to the gain in angular momentum, and when the spin is plotted against the rotational frequency, a **backbend** is seen [103].

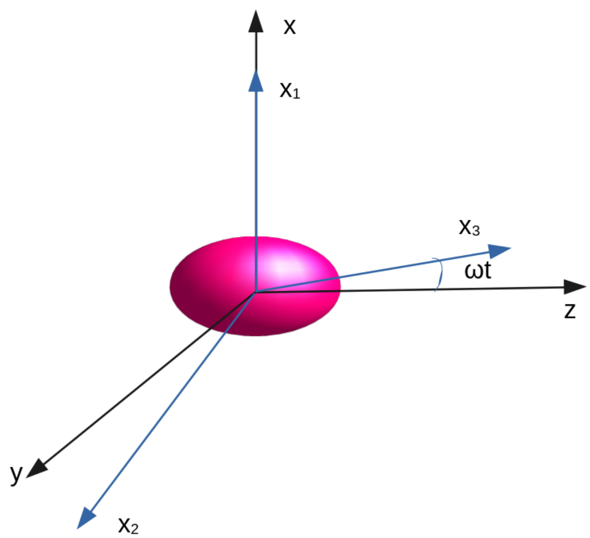

Figure 3.4 Pictorial representation of rotating deformed nucleus. Here, x_1, x_2, x_3 represent the body fixed axes, and x, y, z represent the lab fixed axes.

The movement of the nucleons inside the nucleus was well described by various simplified models. The simplest model is the motion of nucleons in 3D spherical symmetry harmonic oscillator potential. This model generates the single-particle energies of the nuclear orbits, and each state has $(2j + 1)$ degeneracy, where j is the single-particle angular momentum. This degeneracy is removed when an axially symmetric harmonic oscillator potential (Nilsson potential) is included to see the effect of deformation on the single particle orbitals. Each Nilsson state is represented by three asymptotic quantum numbers $\Omega^{\pi}[N,n_z,\lambda]$, where N, n_z and λ represent the total oscillator quantum number, projection of the total oscillator quantum number along the symmetry axis, and the projection of orbital angular momentum on the symmetry axis respectively. Each state can be occupied by a maximum of two particles because the states with a projection of the particle angular momentum j on the symmetry axis with +Ω and -Ω are indistinguishable. When the deformed nucleus rotates faster perpendicular to the symmetry axis, then Coriolis and centrifugal forces will act on the individual nucleon, and an extra term $-\omega I_x$ must be added to the intrinsic Hamiltonian for independent single particle motion. The rotation is treated classically, where the body-fixed system (x_1, x_2, x_3) has a fixed orientation at all times with respect to the nuclear potential. It rotates with rotational frequency ω, relative to the laboratory coordinate system (x, y, z), as shown in Fig. 3.4. The total cranking (rotation) Hamiltonian becomes

$$H_\omega = \Sigma h_\omega = H_0 - \hbar\omega I_x \tag{3.5}$$

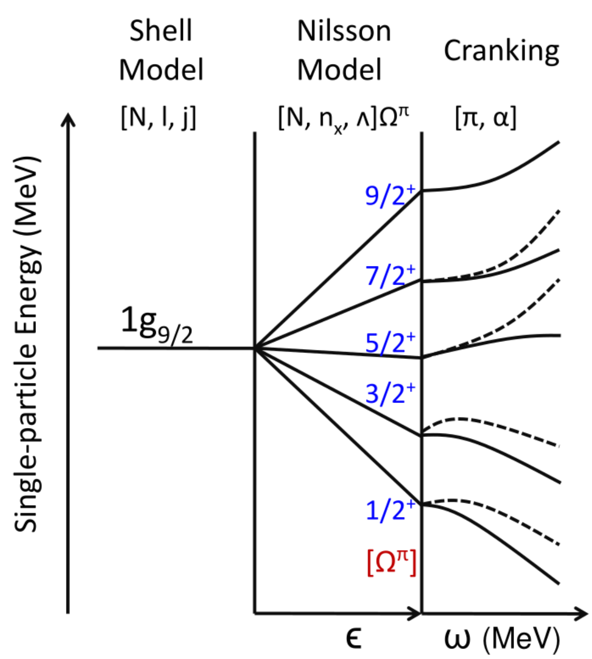

Figure 3.5 The effect of deformed nuclear potential and rotation on $g_{9/2}$ orbital. N, l, and j are the total oscillator quantum number, orbital angular momentum, and angular momentum, respectively. In the case of deformed nuclei, n_x, Λ and Ω are the components of N, l, and j, along the symmetry axis. π and α are the parity and signature quantum numbers in the case of rotating deformed nuclei.

H_0 is a non-rotating Hamiltonian. I_x represents the projection of the total angular momentum onto the rotation axis. This removes the two-fold degeneracy of Nilsson states, and each level is split into two components and represented by two parameters, parity, and signature quantum number (related to invariance of deformed nucleus through 180° with respect to the symmetry axis), as shown on the right side of Fig. 3.5. Thus, the fast nuclear rotation offers the possibility of studying the single-particle spectrum in its full complexity, where all degeneracies are removed. Simplified picture of the particle motion in the hierarchy of various nuclear potentials as described in Fig. 3.5.

The signature quantum number is derived from the rotation operator's eigenvalue. The signature has values 0 or 1 for even nuclei and generates the states:

$$\begin{aligned} I &= 0, 2, 4.....\alpha = 0 \\ I &= 1, 3, 5.....\alpha = 1 \end{aligned} \tag{3.6}$$

and values ±1/2 for odd nuclei, resulting in states :

$$\begin{aligned} I &= 1/2, 5/2, 9/2.....\alpha = 1/2 \\ I &= 3/2, 7/2, 11/2.....\alpha = -1/2 \end{aligned} \tag{3.7}$$

In this thesis, we have used different models depending on the phenomena that have been observed in the nuclei of interest. The detailed description of these models is given in the sections below:

3.2 Large-Scale Shell Model Calculation

The nuclear shell model is successful in describing the low-lying excitation spectra of nuclei near closed-shell nuclei [104]. The nuclear shell model is based on the assumption of the mean-field, where each nucleon moves under an average potential, which can be written as

$$H = \sum_{i=1}^{A} T_i + \sum_{i=1}^{A} V_i + (\sum_{i>j}^{A} \sum_{j=1}^{A} V_{i,j} - \sum_{i=1}^{A} V_i) = H_{sm} + H_{res} \tag{3.8}$$

where $V_{i,j}$ is two-body interaction energy. H_{sm} and H_{res} are the one-body part of the Hamiltonian and the two-body residual interaction part of the Hamiltonian, respectively. After a fruitful success in the nuclear shell model, large-scale shell model (LSSM) computations have been performed to extend the calculations beyond closed-shell nuclei. In the LSSM, we suppose that a nucleus is made up of an inert core and valence particles move in some active orbitals. The nuclear wave function is defined as a superposition of Slater determinants that represent the valence particle's orbital occupations. The construction of a many-body wave function can be done in two ways: J-scheme and M-scheme. J scheme is based on the coupling of angular momentum and becomes computationally expensive as the number of particles increases. The M-scheme focuses on the magnetic quantum number M, which is related to the projection of the total angular momentum J along the rotational symmetry axis. There are several codes that have been developed for the large-scale shell model calculation such as ANTOINE [105], BIGSTICK [106], EICODE [107], KSHELL [108], NATHAN [109], NuSHELL [110], MFDn [111], MSHELL64 [112], OXBASH [113], and VECSSE [114]. For the purpose of the present thesis, the large basis shell model calculation has been performed using KSHELL [108] codes with the SN100PN effective interaction [115].

The simplest representation for a many-body Slater determinant in "M-scheme" basis state can be described as

$$|M_i\rangle = c^{\dagger}_{a_{i,1}} c^{\dagger}_{a_{i,2}} \dots c^{\dagger}_{a_{i,A}} |-\rangle \tag{3.9}$$

where A and $|-\rangle$ represent the number of valence nucleons and an inert core, respectively. The $c_{a_{i,1}}$ is a creation operator for the single-particle state $a_{i,1}$. The slater determinant $|M_i\rangle$ indicates that the first, second, $\cdots$, and Ath particles are in the $a_{i,1}$, $a_{i,2}$,...and $a_{A,1}$

single-particle states, respectively. The set ($a_{i,1}$, $a_{i,2}$, $a_{i,3}$,..., $a_{i,A}$) is sometimes referred to as "configuration".

The shell-model wave function is represented as the linear combination of the M-scheme basis states since they completely span the model space.

$$|\psi\rangle = \sum_{i=1}^{D_M} v_i \, |M_i\rangle \tag{3.10}$$

Where D_M represents the dimension of M-scheme. The coefficient v_i can be obtained by solving the Schrodinger equation.

In the M-scheme basis, two symmetries can be used: rotational symmetry around the z-axis and parity symmetry. The eigen values of rotation (J_z) and parity (Π) operators are M and π , respectively. So, we just need to address a block matrix defined by the M and π. In the case of even-mass nuclei, we must create a subspace with M = 0 that is spanned by the Slater determinants. This subspace has all J states without duplication. In the case of odd-mass nuclei, the M = 1/2 subspace is sufficient to yield all shell model states. Consequently, the antisymmetric product of the single-particle wave functions is obtained, which follows the orthogonality relation.

To perform the LSSM calculation, first, we construct the model space, which includes the inert core and valence proton and neutron orbitals. Finally, we have to choose the effective interaction that will contain the two-body matrix elements (TBME) involving the valence orbitals of the particular model space. The energy eigenvalues are then obtained by diagonalizing the matrix using the effective Lanczos algorithm. The code's output provides the energy eigenstates and eigenvalues together with the percentage contributions of each configuration to the wave function.

3.3 Triaxial Projected Shell Model

The rotational characteristics of deformed nuclei can be described by considering nucleons to move in a deformed potential. Despite recent advances in computer technology, it is nearly impossible to describe medium and heavy-deformed nuclei using the traditional (spherical) shell model. The Nilsson or deformed state is defined in the intrinsic frame of reference in which the rotational symmetry has been broken so that, in order to calculate the observable properties, it is necessary to restore the broken rotational symmetry, which can be done by using the standard angular momentum projection operator [116]. The projection of angular momentum is performed from a chosen set of Nilsson + BCS states close to the Fermi energy, which is utilized to identify the structural characteristics of transitional nuclei. The projected states are then used to diagonalize a shell model Hamiltonian to generate the high-spin excited states of the nuclei. This kind of theoretical approach using the basic philosophy of the shell model is known as the projected shell model (PSM) [117, 118].

Although the projected shell model based on the axial symmetric basis describes many phenomena such as back bending, superdeformed, signature splitting, etc. This model could not explain the moments of inertia for lighter rare-earth nuclei and heavier rare-earth nuclei. The triaxial deformation of $\gamma \approx 30^\circ$ is the only way to explain the sharp increase in moments of inertia of these nuclei as functions of rotational frequency in the low spin region ($I < 10$) [119], as the inclusion of the 2- and higher-quasiparticle bands will not contribute much in this low spin (and low excitation energy) region. It is therefore expected that the moments of inertia and other properties of the transitional nuclei may be described more accurately by using the triaxial basis in the PSM, which requires a three-dimensional angular momentum projection. This approach is known as the triaxial projected shell model (TPSM) [119]. The Hamiltonian consists of the Quadrupole-Quadrupole interaction + monopole pairing + quadrupole pairing force, which is defined as

$$\hat{H}_N = \hat{H}_0 - \frac{\chi}{2}\sum_{\mu}\hat{Q}^{\dagger}_{\mu}\hat{Q}_{\mu} - G_M\hat{P}^{\dagger}\hat{P} - G_Q\sum_{\mu}\hat{P}^{\dagger}_{\mu}\hat{P}_{\mu} \tag{3.11}$$

Where, $\hat{H}_0$ is the spherical harmonic-oscillator single particle hamiltonian while the operators $\hat{Q}$ and $\hat{P}$ are defined as

$$\hat{Q}_{\mu} = \sum_{\alpha\beta} Q_{\mu\alpha\beta} c^{\dagger}_{\alpha} c_{\beta}, \quad \hat{P}^{\dagger} = \frac{1}{2}\sum_{\alpha} c^{\dagger}_{\alpha} c^{\dagger}_{\bar{\alpha}}, \quad \hat{P}^{\dagger}_{\mu} = \frac{1}{2}\sum_{\alpha\beta} Q_{\mu\alpha\beta} c^{\dagger}_{\alpha} c^{\dagger}_{\bar{\beta}},$$

The Hartree-Fock-Bogoliubov (HFB) approximation of the shell model Hamiltonian Eq. 3.11 generates the same quadrupole mean field as the Nilsson potential. Therefore, instead of performing the HFB variational analysis of the Hamiltonian in Eq. 3.11, the Nilsson potential can be directly employed to derive the deformed basis. The final hamiltonian is defined as

$$\hat{H}_N = \hat{H}_0 - \frac{2}{3}\hbar\omega(\varepsilon\hat{Q}_0 + \varepsilon' \frac{\hat{Q}_{+2} + \hat{Q}_{-2}}{\sqrt{2}}) \tag{3.12}$$

where ε and ε' related to the deformation parameter in triaxial nilsson potential. In a more consistent treatment, both ε and ε' have to be varied in order to search for the minimum of the ground state energy.

3.4 Covariant Density Functional Theory

CDFT is an extension of the non-relativistic Density Functional Theory (DFT), which is widely used in condensed matter physics to calculate the properties of complex systems. CDFT [120–123] is built upon Relativistic Mean-Field Theory (RMF), which treats nucleons (protons and neutrons) relativistically, and the nucleons are described as moving in an effective mean-field created by meson exchange like the σ, ω, and ρ meson.

The effective lagrangian density of a nuclear system consists of four parts:

$$\mathscr{L} = \mathscr{L}^{free} + \mathscr{L}^{4f} + \mathscr{L}^{der} + \mathscr{L}^{em} \tag{3.13}$$

where the terms $\mathscr{L}^{free}$, $\mathscr{L}^{4f}$, $\mathscr{L}^{der}$ and $\mathscr{L}^{em}$ represent the free nucleon term, four fermion coupling point, derivative term, and the electromagnetic interaction term, respectively. Each term is defined as:

$$\mathscr{L}^{free} = \bar{\psi}(i\gamma_\mu \partial^\mu - M)\psi \tag{3.14}$$

$$\begin{aligned}\mathscr{L}^{4f} = &-\frac{1}{2}\alpha_S(\bar{\psi}\psi)(\bar{\psi}\psi) - \frac{1}{2}\alpha_{tS}(\bar{\psi}\vec{\tau}\psi)(\bar{\psi}\vec{\tau}\psi)\\ &-\frac{1}{2}\alpha_V(\bar{\psi}\gamma_\mu\psi)(\bar{\psi}\gamma^\mu\psi) - \frac{1}{2}\alpha_{tV}(\bar{\psi}\gamma_\mu\vec{\tau}\psi)(\bar{\psi}\gamma^\mu\vec{\tau}\psi)\\ &-\frac{1}{2}\alpha_T(\bar{\psi}\sigma_{\mu\nu}\psi)(\bar{\psi}\sigma^{\mu\nu}\psi) - \frac{1}{2}\alpha_{tT}(\bar{\psi}\sigma_{\mu\nu}\vec{\tau}\psi)(\bar{\psi}\sigma^{\mu\nu}\vec{\tau}\psi)\\ &-\frac{1}{2}\alpha_{PS}(\bar{\psi}\gamma_5\psi)(\bar{\psi}\gamma_5\psi) - \frac{1}{2}\alpha_{tPS}(\bar{\psi}\gamma_5\vec{\tau}\psi)(\bar{\psi}\gamma_5\vec{\tau}\psi)\\ &-\frac{1}{2}\alpha_{PV}(\bar{\psi}\gamma_5\gamma_\mu\psi)(\bar{\psi}\gamma_5\gamma^\mu\psi) - \frac{1}{2}\alpha_{tPV}(\bar{\psi}\gamma_5\gamma_\mu\vec{\tau}\psi)(\bar{\psi}\gamma_5\gamma^\mu\vec{\tau}\psi)\end{aligned} \tag{3.15}$$

$$\mathscr{L}^{der} = -\frac{1}{2}\delta_S\partial_\mu(\bar{\psi}\psi)\partial^\mu(\bar{\psi}\psi) \tag{3.16}$$

$$\mathscr{L}^{em} = -e\frac{1-\tau_3}{2}\bar{\psi}\gamma_\mu\psi A^\mu - \frac{1}{4}F_{\mu\nu}F^{\mu\nu} \tag{3.17}$$

In this equation, M represents the nucleon mass, e represents the charge unit, and A_μ and $F_{\mu\nu}$ represent the electromagnetic field's four-vector potential and strength tensor, respectively. The subscripts S, V, T, PS, and PV describe the scalar, vector, tensor, pseudo-scalar, and pseudo-vector couplings, respectively. The subscript "t" denotes the corresponding isovector channel.

The Legendre transformation can be used to derive the system's Hamiltonian. The nuclear system's energy density is the expectation value of the Hamiltonian H in the ground-state Slater determinant.

$$E_{CDF} = \langle \Phi_0 | H | \Phi_0 \rangle = E_{kin} + E_{4f} + E_{der} + E_{em}, \tag{3.18}$$

The observed energy density consists of four parts, *i.e.*, the kinetic E_{kin}, four-fermion interaction E_{4f}, derivative E_{der}, and electromagnetic E_{em} parts.

In Covariant Density Functional Theory (CDFT), different types of point coupling models such as PC-PK1 [124], DD-PC1 [125], and PC-F1 [126] are used to describe nuclear interactions. These models avoid the complexity of finite-range interactions and focus on point-like interactions between nucleons. The details of these couplings are given below:

1. **PC-PK1 Coupling (Scalar-Vector Coupling)**

This is the most widely used type of point coupling model. It involves two types of coupling:

Scalar coupling: This coupling describes the interaction in scalar fields, which do not carry spin and are important for explaining the attraction between nucleons.

Vector coupling: This coupling involves vector fields, which are associated with the exchange of virtual particles like mesons, and contribute to the spin-orbit force and other effects.

These types of interactions particularly improve the description of isospin dependence on the binding energy.

2. **PC-F1 Coupling (Scalar-Scalar Coupling)**

This coupling describes the interaction between scalar fields that do not have spin, and the interactions are based on the density of nucleons in a purely scalar fashion. These models focus on the self-interaction of scalar fields, which is often used to describe nuclear matter at high densities.

3. **DD-PC1 Coupling (Density-Depending Coupling)** The DD-PC1 coupling in CDFT refers to a parametrization of the relativistic mean-field theory that includes density-dependent meson-nucleon couplings. This means that the strength of the interactions between the nucleons (protons and neutrons) and the meson fields (such as σ, ω, and ρ mesons) depends on the local nuclear density. This coupling improves the description of nuclear matter, especially at high densities. In the present thesis, we have used the PC-PK1 coupling in CDFT to describe octupole correlations by incorporating octupole deformation into the relativistic mean-field description of the nuclear system.

3.5 Ultimate Cranking Model

The ultimate cranking model [127, 128] is an advanced version of the cranking model, a theoretical framework used in nuclear physics to describe rotating nuclei and their collective motion. This model uses relativistic theories, such as the relativistic mean-field (RMF) theory or the relativistic Hartree-Bogoliubov (RHB) theory, to describe the nuclear system. The ultimate cranking model also typically includes pairing correlations, which are important for properly describing the structure of nuclei, especially for even-even nuclei where paired nucleons form bound states. This model is crucial for understanding the behavior of deformed, rotating, and high-spin nuclei, particularly those far from stability or in exotic regions of the nuclear chart.

A general form of the Hamiltonian for the cranking model could be:

$$\hat{H} = \hat{H}_0 + \hat{H}_{rot} + \hat{H}_{pair} \tag{3.19}$$

where,

(1) $\hat{H}_0$ is the intrinsic single particle Hamiltonian by considering the Nilsson mean field potential.

(2) $\hat{H}_{rot}$ represent the rotational energy of the nucleus.

$$\hat{H}_{rot} = \frac{\hat{J}^2}{2\mathscr{J}} \tag{3.20}$$

where $\hat{J}$ is the angular momentum operator and $\mathscr{J}$ is the moment of inertia, which depends on the nuclear deformation.

(3) $\hat{H}_{pair}$: Relativistic Hartree-Bogoliubov (RHB) equations are used to address the pairing interaction in the relativistic cranking model. The relativistic pairing term is commonly expressed as follows:

$$\hat{H}_{pair} = \sum_{k,k'} (G_{k,k'} \hat{\Phi}_k^\dagger \hat{\Phi}_{k'}) \tag{3.21}$$

where, $\hat{\Phi}_k$ is the quasiparticle field operator for the single-particle state, and $G_{k,k'}$ is the pairing interaction strength (which depends on the type of nucleon—proton or neutron). This model also includes the higher-order deformation term beyond axial deformation, such as the octupole and triaxial term and Strutinsky shell correction.